



# Influence of urban forest size and form on PM<sub>2.5</sub> and O<sub>3</sub> concentrations: A perspective of size threshold

Xin Chen<sup>1</sup> · Fang Wei<sup>1</sup>

Received: 20 November 2024 / Accepted: 11 February 2025  
© The Author(s), under exclusive licence to Springer Nature B.V. 2025

## Abstract

Urban forest (UF) is an effective means of mitigating air pollution. At the stage where PM<sub>2.5</sub>-O<sub>3</sub> composite pollution is prevalent and UF expansion reaches a bottleneck, optimizing UF form based on its area size becomes a superior management strategy. However, existing research has not fully explored the threshold effects of UF size. Using the panel threshold regression model, this study examines relationships between air pollution and UF (size and form) in 305 counties within the Yangtze River Delta (YRD) from 2014 to 2022. The results show (1) UF size exhibits a double threshold effect in three relationships: between patch density (PD) and PM<sub>2.5</sub>, between splitting index (SPLIT) and PM<sub>2.5</sub>, and between SPLIT and O<sub>3</sub>. Meanwhile, a single threshold effect of UF size is observed in relationships between other UF form metrics and pollutant concentrations. (2) When UF size plays the threshold effect in relationships between UF form and pollutant concentrations, its threshold values usually lie around 3%, 14%, and 45%. UF form metrics' correlations with PM<sub>2.5</sub> are generally opposite to those with O<sub>3</sub>. (3) When UF size is below 45%, PM<sub>2.5</sub> reduction favors complex-shaped and dispersed UF patches, while O<sub>3</sub> reduction benefits from more regular and concentrated UF patches. Once UF size exceeds 45%, a continuous regional UF network can potentially address PM<sub>2.5</sub>-O<sub>3</sub> composite pollution. This study aims to provide insights into atmospheric governance and UF planning.

**Keywords** PM<sub>2.5</sub>-O<sub>3</sub> composite pollution · Urban forest · Size and form · Threshold effect · Panel threshold regression model · The Yangtze River Delta

## Introduction

Extensive development has severely damaged the atmospheric environment in China (Duan et al. 2022). PM<sub>2.5</sub> pollution emerged as the main concern in the early 2010s. In response, the Chinese government has implemented a series of Air Clean Acts, among which end-of-pipe management is one important strategy (Xiao et al. 2020; Han et al. 2022; Li et al. 2023b). Consequently, on the one hand, PM<sub>2.5</sub> concentration has decreased but remains above the guideline level set by the WHO 2021 Global Air Quality Guidelines; O<sub>3</sub> concentration has significantly increased, surpassing the

guideline level; other pollutant concentrations (including SO<sub>2</sub>, NO<sub>2</sub>, and CO) have decreased and now fall below the guideline levels (Lin et al. 2022). That is, PM<sub>2.5</sub>-O<sub>3</sub> composite pollution has become the foremost issue affecting the atmospheric environment in China (Zhang et al. 2022; Wu et al. 2024). On the other hand, the marginal effect of end-of-pipe management has been diminishing, thereby new approaches to effectively control atmospheric pollution should be proposed (Zhao et al. 2021; Li et al. 2023a). Among them, optimizing land-use patterns has been recognized as a valuable supplement, achieved by directly influencing the ecological effect of land and human activities on the land (Lu et al. 2020; Chen and Wei 2024).

Urban forest (UF) is a critical land type, covering all vegetation across a city's urban–rural continuum and serving as a key natural component of the city (Konijnendijk 2003; Wang et al. 2024). It offers multiple benefits and is regarded as a nature-based solution for improving the ecological environment (Chen and Li 2021; Feng and Fang 2022). The role of UF in mitigating PM<sub>2.5</sub> pollution has

✉ Xin Chen  
3180104697@zju.edu.cn

Fang Wei  
weif@zju.edu.cn

<sup>1</sup> College of Civil Engineering and Architecture, Zhejiang University, No.866 Yuhangtang Road, Xihu District, Hangzhou, Zhejiang, China

been widely studied (Zheng et al. 2019). Unlike construction land and cropland, UF has relatively few particulate matter emission sources and exhibits a stronger capacity to capture particles. Additionally, vegetation in the UF can absorb and degrade particulate matter while regulating the local microclimate, further influencing PM<sub>2.5</sub> concentrations (Lu et al. 2020; Shen et al. 2023). Moreover, the impact of UF on ozone has also been observed. UF can directly enhance the dry deposition of ozone and indirectly inhibit ozone formation by reducing particles (Zhang et al. 2020; Qu et al. 2023). However, vegetations in the UF also emit ozone precursors such as biogenic volatile organic compounds (BVOCs), indirectly contributing to higher O<sub>3</sub> concentrations (Zhu et al. 2019; Qu et al. 2023). These make the relationship between UF and O<sub>3</sub> concentration more complex than that with PM<sub>2.5</sub> concentrations. Furthermore, complex chemical interactions exist between PM<sub>2.5</sub> and O<sub>3</sub> (Zhao et al. 2023). PM<sub>2.5</sub> could affect O<sub>3</sub> by altering aerosol-photolysis rates and participating in heterogeneous reactions, thereby either inhibiting or promoting ozone production under various conditions (Wu et al. 2021; Qu et al. 2023). Meanwhile, O<sub>3</sub> could influence the atmospheric oxidizing capacity and atmospheric photochemical reactivity, thereby affecting the formation of secondary PM<sub>2.5</sub> (Pathak et al. 2009; Li et al. 2012). Therefore, the impacts of UF on PM<sub>2.5</sub> and O<sub>3</sub> should be identified and analyzed comparatively, which is seldom explored in existing research.

Afforestation has been a long-standing initiative in China. The National Forest City action has been launched since 2004, which essentially aims to achieve sustainable development goals (Wang et al. 2024). Additionally, the protection and restoration of ecological spaces hold a highly prioritized position within the Chinese territorial spatial planning system under the guidance of ecological priority (Liu et al. 2018; Liu and Zhou 2021), thereby UF (as an important type of ecological land) receives more attention. However, a series of policies, regulations, and social practices have primarily focused on the UF size indicators (Xu et al. 2020), while largely neglecting UF form metrics. Indeed, size and form are two important aspects of UF spatial patterns. Size reflects the area status of UF, usually represented by the proportion of UF area in the total territorial area; Form is the spatial geometric characteristics of UF, such as aggregation and shape complexity (Shih 2017; Mo et al. 2019). In academic research, scholars have studied pollutant concentrations' correlations with both UF and green space in urban built-area from the perspective of either size or form (Cai et al. 2020; Cao et al. 2024). UF encompasses all vegetation across the urban–rural continuum, making its size and form more readily monitored and adjusted. To facilitate the practical application of research insights, further study should be conducted from the perspective of both size and form.

Complex interrelationships exist between UF size and form (Mo et al. 2019; Silveira et al. 2024). Evolution in UF size will simultaneously lead to changes in UF form, thereby influencing UF's ecological benefits (Fan et al. 2019). Studies have found that without enlarging UF sizes, optimizing UF forms could also result in better pollution-mitigation effects. For example, Wang et al. (2022) found that increasing the shape complexity of forests in China led to a reduction in PM<sub>2.5</sub> concentrations. Additionally, when UF size exceeds a certain value, UF's ability to reduce pollutants will experience dramatic shifts, which is the threshold effect of UF size (Yu et al. 2020). For example, Zhou et al. (2019) found that forests would better reduce PM<sub>2.5</sub> since their coverage surpasses 30% in construction land or 60% along the periphery of urban metropolitan development zone. Similarly, it can be inferred that correlations between UF form characteristics and pollutant concentrations vary significantly across various UF size intervals. Understanding this phenomenon can provide a reference for optimizing UF form to strengthen UF's ability to reduce pollutants when UF size expansion reaches a saturation state. However, while threshold effects of UF size on its form's ecological benefits have been observed in studies on UF cooling (Kong et al. 2014; Peng et al. 2020), such effects have not been explored in the context of atmospheric pollution reduction. Therefore, further research is needed in the area of pollution mitigation.

To fill research gaps, this study takes 305 counties within the Yangtze River Delta as research units, with both forest and shrub being treated as UF. The panel threshold regression model is then utilized to analyze the threshold effect of UF size on its pollution-mitigation ability. This study proposes that UF size owns threshold effects on the pollution reduction ability of UF form. Based on the hypothesis, optimizing the UF form based on its size threshold could effectively supplement atmospheric governance and UF planning. The marginal contribution of this study lies in (1) This study focuses on the pollution reduction effects of UF form at different UF sizes, which is more in-depth than just exploring the linear relationships between pollutant concentrations and UF form; (2) This study explores and compares the impacts of UF patterns on both PM<sub>2.5</sub> and O<sub>3</sub> concentrations, which is more in line with the realities of atmospheric governance in China; (3) This study sets the county as the basic unit, which is also the minimum legal unit of overall planning in Chinese territorial spatial planning system, thus facilitating the integration of UF form metrics into planning practices. This study aims to provide theoretical references and practical support for managing the atmospheric environment, protecting and restoring urban forests, and territorial spatial planning.

## Materials and methods

### Study area and period

The Yangtze River Delta (YRD) is situated along the eastern coast of China (Fig. 1), covering four provinces in the lower reaches of the Yangtze River: Shanghai, Jiangsu, Zhejiang, and Anhui. The reasons for selecting the YRD as the study area are as follows: Firstly, the YRD is one of the most prosperous regions in China in terms of socio-economic development, while also facing severe PM<sub>2.5</sub>-O<sub>3</sub> composite pollution after rapid urbanization and intense industrialization (Lin et al. 2022; Qu et al. 2023). Secondly, the YRD features diverse UF sizes across different areas, with mountainous and hilly terrain in the southwest and vast plains in the central and northern regions (Li et al. 2023c). Finally, the entire YRD is located in the subtropical monsoon climate zone (An et al. 2023), thereby the similar meteorological conditions and vegetation characteristics help minimize the potential interference with the study results. Besides, since this study is practice-oriented and spatial big data used are independent of administrative boundaries, 305 counties within the YRD are selected as research units.

Given that China has gradually entered the PM<sub>2.5</sub> and O<sub>3</sub> composite pollution stage following the implementation of the Air Pollution Action Plan launched in 2013 (Du et al. 2024), this study selects the years from 2014 to 2022 as the study period. Due to shifts in economic development strategies and adjustments in spatial planning systems, land use patterns in the YRD, including UF size, also experienced

significant changes during this period (Zhou and Wang 2022), demonstrating the research potential.

### Panel threshold regression model

Introduced by Tong (1983) and innovated by Hansen (1999, 2000), the panel threshold regression model can divide samples into several distinct groups with estimated thresholds, thereby allowing for regressing separately and gaining a more fine-grained understanding of the nonlinear correlations between elements. It was first widely used in socio-economic fields (Chen et al. 2013; Deng et al. 2014), while its application in environmental domains has been gradually attempted in recent years (Ouyang et al. 2019; Deng et al. 2024). This study takes it to explore the threshold effects of UF size on UF form's pollution reduction ability. The formulas are as follows:

$$Y_{it} = \beta_0 R_{it} + \theta_1 X_{it} \cdot I(q_{it} \leq \gamma_1) + \dots + \theta_k X_{it} \cdot I(\gamma_{k-1} < q_{it} \leq \gamma_k) + \dots + \theta_{n+1} X_{it} \cdot I(\gamma_n < q_{it}) + \mu_i + \varepsilon_{it} \quad (1)$$

$$I(con) = \begin{cases} 1, & con = True \\ 0, & con = False \end{cases} \quad (2)$$

In Eq. (1),  $Y_{it}$  represents the dependent variable of unit  $i$  at time  $t$ ,  $\mu_i$  represents the individual effect,  $\varepsilon_{it}$  is the error term;  $X_{it}$  represents the core explanatory variable of unit  $i$  at time  $t$ ,  $R_{it}$  represents a set of independent variables except  $X_{it}$  of unit  $i$  at time  $t$ ,  $\beta_0$  and  $\theta_k$  are corresponding coefficients.  $q_{it}$  is the threshold variable of unit  $i$  at time  $t$ ,  $\gamma_k$  represents the  $k$ -th threshold value;  $I(con)$  is the indicator function (as

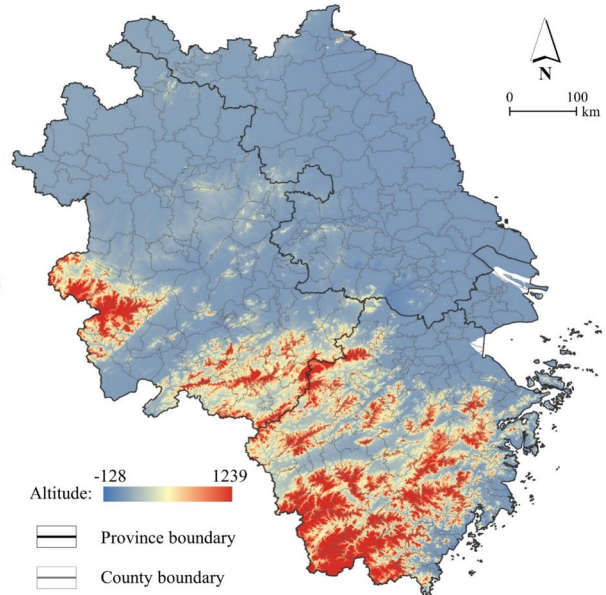
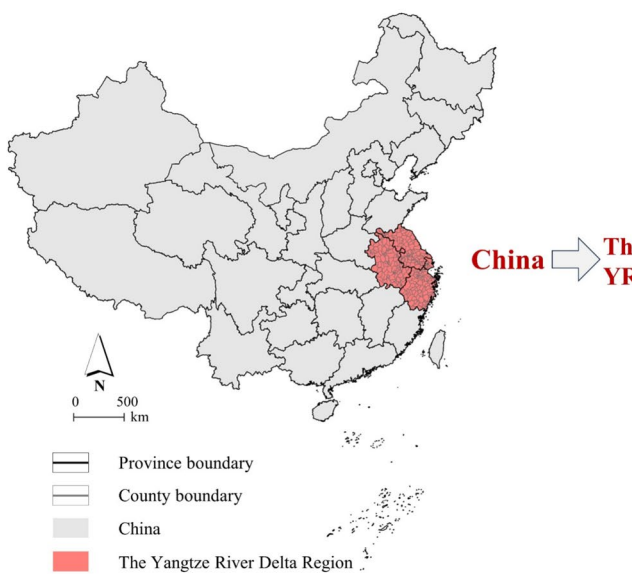


**Fig. 1** Location of the YRD and research units in it

detailed in Eq. (2)): It equals 0 when *con* is false, while equals 1 when *con* is true.,

The threshold value  $\gamma$  is first determined when the residual sum of squares (RSS) of the fitting model is minimized, with successively taking sample values as candidate thresholds and estimating  $\theta_k$  by least squares estimation (Huo et al. 2021). Then the bootstrap method is used to calculate the F\_statistic and P\_value to determine the significance of the threshold effect. Subsequently, the likelihood ratio (LR) statistic (as shown in Eq. (3) and the 95% confidence intervals are calculated to examine the authenticity of the estimated threshold value (Hansen 1999).

$$LR(\gamma) = \frac{RSS(\gamma) - RSS(\hat{\gamma})}{RSS(\hat{\gamma})/N(T-1)} \quad (3)$$

In Eq. (3),  $\hat{\gamma}$  is the estimation of  $\gamma$ ;  $N$  represents the number of samples per year, and  $T$  represents the timespan.

## Variables and data

### Dependent variables

$PM_{2.5}$  concentration ( $PM_{2.5}$ ) and  $O_3$  concentration ( $O_3$ ) are set as two dependent variables and regressed separately on the other independent variables. In line with atmospheric pollutant indicators and relevant studies (Wu et al. 2024),  $PM_{2.5}$  is represented by the annual average of  $PM_{2.5}$  concentration, while  $O_3$  is represented by the yearly average of daily maximum 8-h  $O_3$  concentration.  $PM_{2.5}$  and  $O_3$  data are obtained from ChinaHighAirPollutants (CHAP) datasets developed by Wei and Li (2021, 2022), with a spatial resolution of 1 km\*1 km. Among CHAP datasets, the  $PM_{2.5}$

dataset is built on the satellite-based MODIS MAIAC AOD product, while the  $O_3$  dataset is mainly predicted by downward shortwave radiation and air temperature. For both datasets, artificial intelligence techniques are utilized to integrate various auxiliary data to inverse full-coverage maps. These auxiliary data include meteorological variables, surface conditions, pollutant emissions, and population distribution, which are obtained from sources such as ground-based observations, atmospheric reanalysis, and emission inventories. Consequently, ten-fold cross-validation  $R^2$  for  $PM_{2.5}$  and  $O_3$  presents 0.92 and 0.89, respectively.

### Threshold variable and core explanatory variables

UF size is designated as the threshold variable, while UF form serves as the core explanatory variable. Landscape metrics derived from landscape ecology knowledge are utilized to quantify UF size and form. According to relative studies (Peng et al. 2016; Zhou et al. 2019), UF size is quantified by the proportion of UF area within the county (PFO). UF form is quantified by six landscape metrics, which are selected based on these principles concerning relative studies (Zhao and Huang 2022; Ran et al. 2023): effectively depicting spatial characteristics of the land, such as shape and distribution; being easy to calculate and monitor in practice; and applying to all counties. All UF size and form metrics selected and their detailed information are presented in Table 1. All metrics are calculated by Fragstats 4.2.

UF data is derived from Land-use data (30 m\*30 m) provided by the China Land Cover Dataset (CLCD). Considering that forests and shrubs are the main integrators of vegetation in a region and that shrubs are an important part of the forest system with similar ecological benefits to forests

**Table 1** UF size and form metrics chosen in the study

Type	Metric	Definition and significance	Unit	Abbreviation
UF size	Proportion of UF area in the county	Reflecting the dominance of UF in the total area of the county. When the value is higher, the UF size is larger	%	PFO
UF form	Area weighted mean shape index	The value of dividing the mean UF patch perimeter by the minimum perimeter possible for the same area; When the value is higher, the shape of UF patches is more irregular	-	AWMSI
	Patch density	The number of UF patches per unit area; When the value is higher, the distribution of UF patches is more fragmented	1/hm <sup>2</sup>	PD
	Splitting index	The number of subdividing the county area into patches with the same area-weighted mean UF patch area; The higher value means being more separated	-	SPLIT
	Contagion	Reflecting the natural connectivity of UF patches; The higher value means being more contagious	%	CONTAG
	Aggregation index	The number of dividing adjacencies of UF patches by the maximum possible adjacencies of UF patches; The higher value means being more aggregated	%	AI
	Patch cohesion index	Reflecting the tendency of UF to be aggregated; When the value is higher, the distribution of UF patches is more cohesive	%	COHESION

(Toledo-Garibaldi et al. 2023; Yang et al. 2024), both forest and shrub in nine land-use types (Fig. 2a) are treated as UF in this study. To produce CLCD, Yang and Huang (2023) collected the training samples by combining stable samples extracted from China's land-use/cover datasets (CLUDs) and visually interpreted samples from satellite time-series data. Then with these samples, over 335 thousand Landsat images on the Google Earth Engine platform were used to classify national land into 9 types by the random forest model. Methods including spatiotemporal filtering and logical post-processing are utilized to examine and improve the accuracy of classification. Consequently, the overall classification accuracy reaches 79.31%.

### Control variables

Three types of control variables are selected according to relevant studies on factors influencing air pollution (Hu et al. 2017; Chen and Wei 2024): built environment factors, socioeconomic factors, and meteorological factors. Socioeconomic factors primarily reflect and adjust human activities, thereby influencing air quality. Built environment and meteorological factors directly impact the dispersion and concentration of air pollutants and indirectly affect pollutant emissions through their interaction with human activities (Lu et al. 2021; Liu et al. 2022).

Specific indicators belonging to different control variable types are further selected. Kernel density of road crossings (ROA) and proportion of construction land area (PCL) are selected to represent the built environment; Nighttime light

intensity (NTL) and permanent population density (POP) are selected to represent socioeconomic development; Precipitation (PRE) and Temperature (TEM) are selected as meteorological factors.

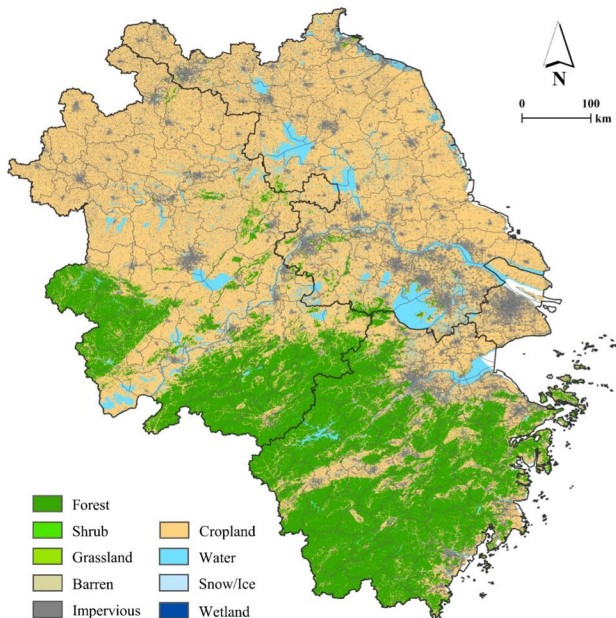
Regarding data sources: Road crossing data is obtained from OpenStreetMap (<https://www.openstreetmap.org/>). Construction land data is extracted from the previously mentioned land-use data. Night light data (1 km\*1 km) is obtained from NPP/VIIRS night light data on the Earth Observation Group platform (<https://eogdata.mines.edu/>); Permanent population data (1 km\*1 km) is obtained from the LandScan population dataset (<https://landscan.ornl.gov/>); Precipitation and temperature data (1 km\*1 km) are obtained from the Third Pole Environment Data Center Platform (TPDC, <https://data.tcdc.ac.cn/>). Besides, county zoning data is from the Resource and Environment Data Cloud Platform (<https://www.Resdc.cn/>).

## Results

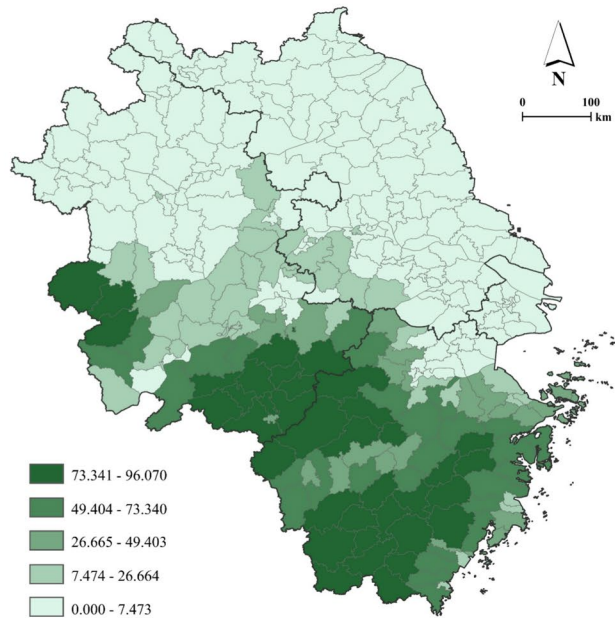
### Territorial space and distribution of UF sizes in the YRD

Table S1 presents the overall numerical performance of UF size and form metrics during the study periods. It can be seen that the forests of counties within the YRD have undergone relatively slight changes over time. Specifically, UF sizes have gradually declined, although the decrease remains within 1%, and the PFOs across different counties have

a. Territorial space



b. Distribution of PFOs



**Fig. 2** Territorial space and distribution of UF sizes in the YRD in 2022. Note: Both forest and shrub are treated as UF in the study

gradually converged. Regarding UF form, AWMSI increased before 2018 and decreased after that; PD decreased before 2018 and then increased; SPLIT has significantly declined; CONTAG has shown increased fluctuationally; and COHESION has grown, though the increase is limited to within 1%.

Furthermore, the territorial space and UF sizes (quantified by PFOs) of each county in the year 2022 are taken for example, as shown in Fig. 2. Forests and shrubs have formed three clusters in the YRD: Western Anhui, the border area of Anhui and Zhejiang, and southern Zhejiang. Counties in these areas overall have relatively higher UF sizes. In contrast, areas in the northern YRD, including Jiangsu, northern Anhui, and Shanghai, are mainly vast plains consisting of cropland and waters, thereby owning smaller UF sizes.

## Spatiotemporal distribution of PM<sub>2.5</sub> and O<sub>3</sub> concentrations

Figure 3 shows the changes in PM<sub>2.5</sub> and O<sub>3</sub> concentrations, along with their Pearson correlation, over the study period. It can be observed that the PM<sub>2.5</sub> concentration generally exhibits a downward trend, while the O<sub>3</sub> concentration fluctuates upward, as indicated by the mean, median, and extreme values. Qi et al. (2023) have found urbanization's inverted "U-shaped" and "U-shaped" nonlinear relationships with PM<sub>2.5</sub> and O<sub>3</sub> concentrations respectively in China. The YRD is highly urbanized and research units are all in the middle or late stages of urbanization, so the phenomenon meets Qi's conclusion. Besides, the Pearson correlation between PM<sub>2.5</sub> and O<sub>3</sub> concentrations changed to be positive and increased dramatically from 2015 to 2018. Though the coefficient has fluctuated and slightly decreased since 2018, it has consistently reflected strong correlations between PM<sub>2.5</sub> and O<sub>3</sub> concentrations since 2017 (with coefficients larger than 0.6). This suggests that controlling one pollutant

can directly affect the other, indicating that PM<sub>2.5</sub> and O<sub>3</sub> can be treated as governance objects simultaneously.

Furthermore, the spatial distribution of PM<sub>2.5</sub> and O<sub>3</sub> concentrations in the YRD for the year 2022 is visualized in Fig. 4. PM<sub>2.5</sub> concentrations form a high-value core in the northwest YRD, with a near-circular decreasing pattern towards the southeast. Meanwhile, O<sub>3</sub> concentrations show a high-value core in Jiangsu, with elevated O<sub>3</sub> concentrations in the counties at the borders of Shanghai, Zhejiang, and Anhui. Lower O<sub>3</sub> concentrations characterize other areas in Zhejiang and Anhui. Both pollutant concentrations overall are characterized by higher values in the north and lower values in the south, with spatial clustering showing some consistency with the land-use patterns and distribution of UF sizes in the YRD.

## Threshold effects of UF size

### Collinearity analysis for variables

Regarding collinearity analysis, the variance inflation factors (VIF) of independent variables are calculated with results shown in Table 2. In the first round, the VIFs of COHESION, AI, PCL, and NTL were all greater than 10. AI, which had the highest VIF, was removed, and the VIFs for the remaining variables were recalculated. Similarly, PCL was excluded in the second round. In the third round, the remaining variables all had VIFs below 10, so they were included in the subsequent regression analysis.

### Test results of threshold existence

First, the existence of the threshold effect of UF size (quantified by PFO) on the pollution reduction effects of UF form was tested, and the results are presented in Table 3. In the PM<sub>2.5</sub> fitting model, PFO exhibits a single threshold effect on

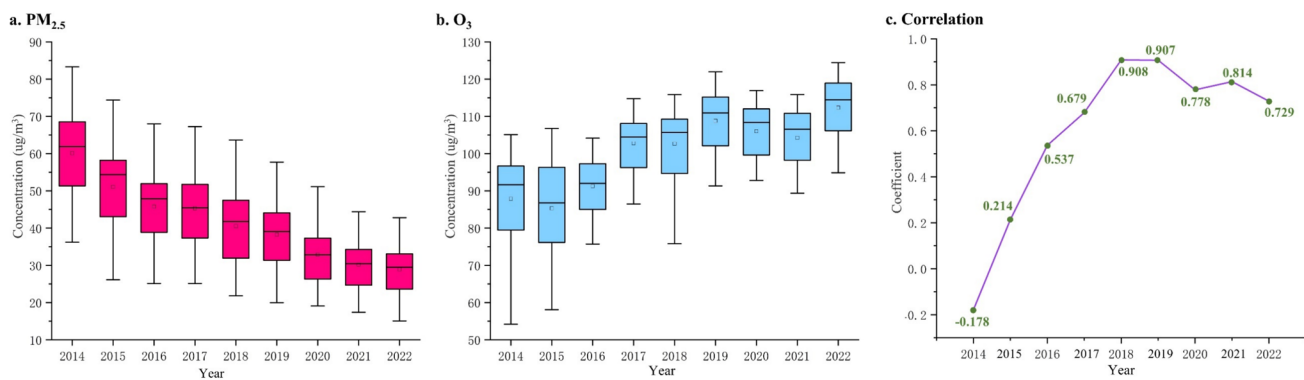


**Fig. 3** Temporal evolution of two pollutant concentrations and their Pearson correlations. Note: (1) Fig. 3a and b are box plots of PM<sub>2.5</sub> and O<sub>3</sub> concentrations, respectively; (2) Coefficients of Pearson cor-

relations in Fig. 3c all have passed the significance tests, reflected by P-values less than 0.01

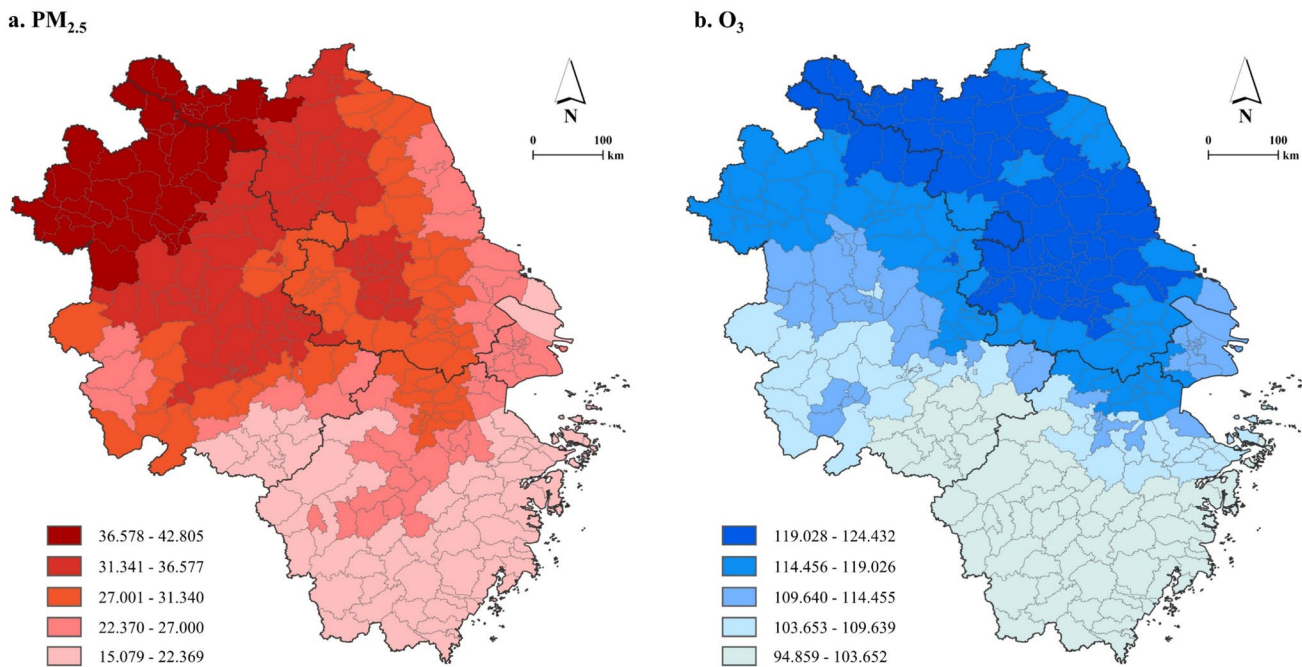


**Fig. 4** Spatial distribution of PM<sub>2.5</sub> and O<sub>3</sub> concentrations in 2022

**Table 2** Results of VIF tests for independent variables

Variable	VIF in round 1	VIF in round 2	VIF in round 3
PFO	5.763	5.204	4.999
AWMSI	3.762	3.753	3.740
PD	1.433	1.428	1.408
SPLIT	1.046	1.043	1.042
CONTAG	1.331	1.325	1.289
COHESION	13.165	1.858	1.803
AI	15.242	-	-
ROA	1.799	1.799	1.761
PCL	11.293	10.907	-
NTL	10.280	10.252	4.288
POP	3.791	3.732	3.360
PRE	3.056	3.051	2.989
TEM	1.666	1.656	1.656

AWMSI and COHESION, while the double threshold effects on PD and SPLIT are also observed. In the O<sub>3</sub> fitting model, PFO demonstrates a single threshold effect on AWMSI, PD, and COHESION, while a double threshold effect is observed for SPLIT. Additionally, in the fitting models for both PM<sub>2.5</sub> and O<sub>3</sub>, PFO shows no threshold effect on CONTAG.

Furthermore, the validity of the thresholds and their effects was tested using 95% confidence intervals (as shown in Table 3) and LR statistics (as illustrated in Fig. 5). It can be seen that the 95% confidence intervals corresponding to the selected thresholds are all in the smaller range and pass

the test. Noticeably, when PFO is used as the threshold variable in the PM<sub>2.5</sub> fitting model, its second threshold for PD and SPLIT, as well as the single threshold for COHESION, is the same at 45.228%; its first threshold for PD and SPLIT are also quite close, at 3.105% and 3.136%, respectively. When PFO is used as the threshold variable in the O<sub>3</sub> fitting model, its single thresholds for PD and COHESION, as well as the first threshold for SPLIT, are close, at 3.409%, 3.331%, and 3.062%, respectively. Additionally, the thresholds of PFO for reducing the concentrations of both pollutants through AWMSI are close, at 13.887% when fitting PM<sub>2.5</sub> and 14.741% when fitting O<sub>3</sub>.

### Results of panel threshold regression models

Next, the regression results for pollutant concentrations and different UF form metrics under the influence of the threshold variable (PFO) were calculated, as shown in Tables S2 and S3. The coefficients representing the relationship between specific UF form metrics (used as core explanatory variables) and pollutant concentrations across different PFO intervals are presented in Table 4.

As UF size increases, the UF form metrics exhibit distinctly opposite performances when fitting PM<sub>2.5</sub> and O<sub>3</sub> concentrations. Specifically, as the size of UF increases, the effectiveness of UF form metrics in mitigating PM<sub>2.5</sub> concentrations intensifies. Among them, AWMSI shifts from a positive correlation with PM<sub>2.5</sub> concentration to a negative correlation, indicating a shift from promoting

**Table 3** Results of threshold effects of UF size on UF form metrics

Pollutant	Core explanatory variable (UF form metric)	Threshold type	F_ statistic	Threshold value (UF size, PFO)	95% confidence interval
PM <sub>2.5</sub>	AWMSI	Single	105.860*	13.887	[3.253, 14.741]
		Double	71.689		
	PD	Single	70.230**	3.105,	[2.971, 3.253],
		Double	50.777*	45.228	[44.755, 45.615]
	SPLIT	Triple	27.704		
		Single	54.874*	3.136,	[2.890, 3.331],
		Double	43.064*	45.228	[44.701, 45.704]
	CONTAG	Triple	25.732		
		Single	30.475	-	-
		COHESION	Single	56.569*	45.228
	O <sub>3</sub>	Double	48.628		[44.701, 45.704]
		AWMSI	Single	89.052***	14.741
		Double	31.099		[13.685, 15.714]
O <sub>3</sub>	PD	Single	59.175**	3.409	[3.112, 3.530]
		Double	22.232		
	SPLIT	Single	56.587*	3.062, 18.109	[2.876, 3.253]
		Double	44.044*		[4.124, 18.893]
		Triple	44.429		
	CONTAG	Single	17.171	-	-
		COHESION	Single	46.117*	3.331
	COHESION	Double	36.065		[3.054, 3.514]

(1) This study determines the threshold type by incrementing the number of thresholds one at a time starting with a single threshold and stopping the increment when the threshold type is not significant; (2) Regarding the significance level, \* represents  $P_{\text{value}} < 0.1$ ; \*\* represents  $P_{\text{value}} < 0.01$ ; \*\*\* represents  $P_{\text{value}} < 0.001$

to absorbing PM<sub>2.5</sub>; The correlation coefficient between PD and PM<sub>2.5</sub> concentration remains positive, although its absolute value decreases; The correlation between SPLIT and PM<sub>2.5</sub> shifts from positive to negative once PFO crosses the first threshold, and the absolute value of this negative coefficient increases as PFO exceeds the second threshold; The pollution reduction effect of COHESION becomes apparent as PFO enters the second interval, as evidenced by a significant negative coefficient. Conversely, the ability of UF form metrics to reduce O<sub>3</sub> diminishes as UF size increases into larger intervals. Specifically, AWMSI shifts from inhibiting ozone formation to promoting it as PFO crosses the threshold; The absolute value of the negative coefficient between PD and O<sub>3</sub> concentration decreases after PFO crosses the threshold; The correlation between SPLIT and O<sub>3</sub> changes from negative to positive after PFO exceeds the first threshold, with the positive coefficient intensifying after PFO surpasses the second threshold; O<sub>3</sub> reduction effect of COHESION becomes evident as PFO enters the second range, which is indicated by a significant negative coefficient.

## Discussion

### Potential reasons for the threshold effect of UF size

This study observed a threshold effect of UF size on atmospheric pollution reduction, providing additional evidence for the threshold effect of UF size in promoting ecological benefits (Peng et al. 2016; Fan et al. 2019). To understand the phenomenon, scale effects and diminishing marginal returns have been proposed as possible explanations. Specifically, when the UF size is small, the vegetation has a limited capacity to influence pollutants on an individual basis. Once the UF size reaches a critical threshold, the vegetation can form an integrated system, interacting more effectively with pollutants (Lin et al. 2020), which results in a qualitative change in its relationship with them. However, beyond a certain point, the marginal benefit of further increasing UF size diminishes (Vaz Monteiro et al. 2016). This can be attributed to the following reasons: (1) As the UF area increasingly occupies a larger proportion of the

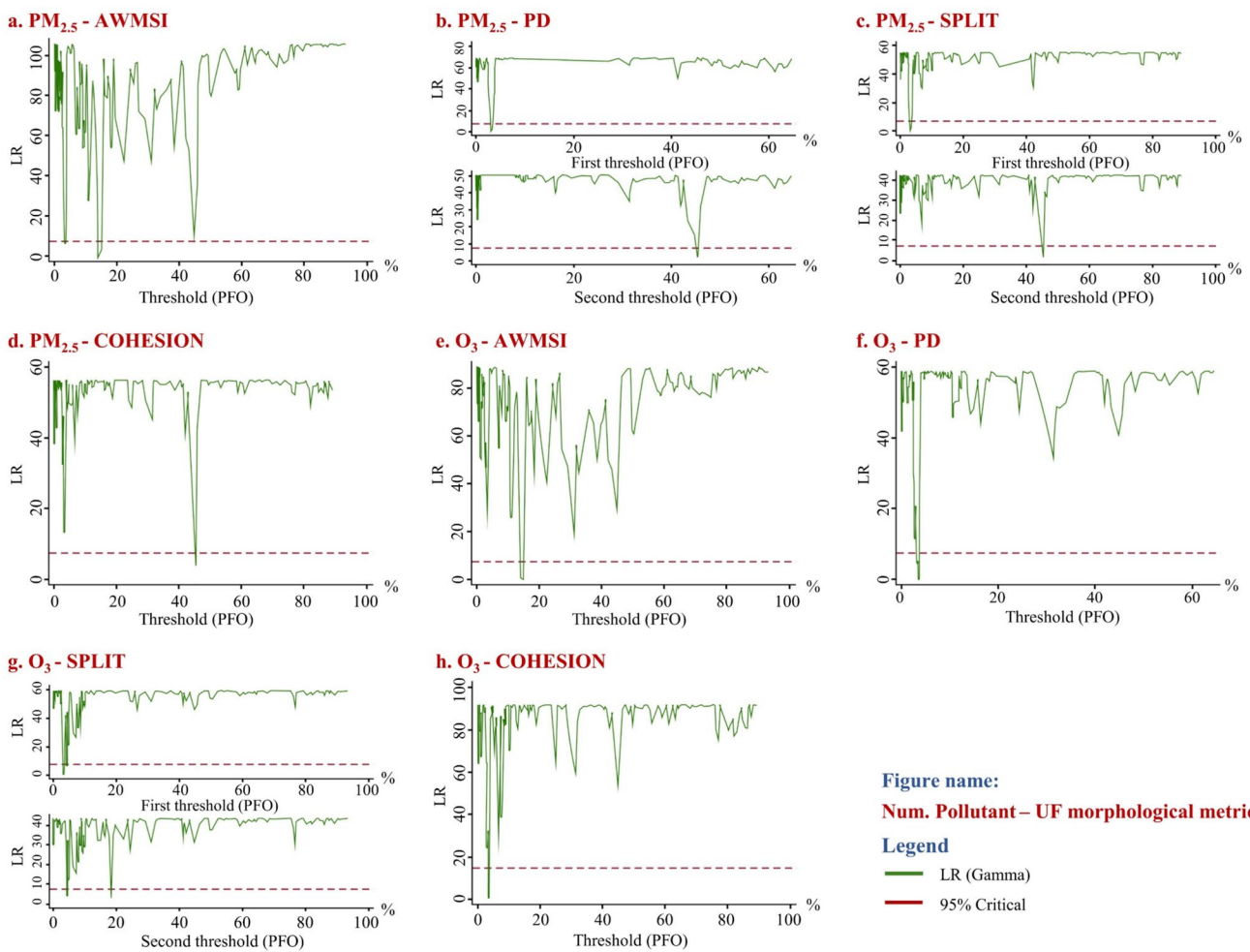


**Fig. 5** LR diagrams with the threshold variable PFO

unit, the available space for further UF expansion diminishes; (2) As pollution levels are reduced, fewer pollutants remain to be treated (Escobedo and Nowak 2009); (3) The overall pollution abatement capacity of vegetation is also limited (Hu et al. 2020), which cannot continue to grow indefinitely. Overall, under the combined effects of scale effects and diminishing marginal returns, UF size exhibits threshold effects on UF's pollution reduction performance.

As mentioned above, UF exhibits varying pollution reduction potentials at different sizes. It can be further inferred that the specific UF form influences the degree of UF's functioning. This suggests that at different UF sizes, the pollution reduction capacity of UF will exhibit a specific tendency related to its form. This interpretation illustrates the threshold effect of UF size on the relationship between UF form and pollutant concentrations. Specifically, on the one hand, UF form can affect the overall integrity of the UF (Li et al. 2023d), with a tightly packed UF more likely to exert its scale effect and reach the critical threshold for diminishing marginal benefits earlier; On the other hand,

UF form affects the degree of interaction between the UF and other spaces (Zhai et al. 2022), thereby amplifying the source/sink role of the UF at the corresponding sizes. Nevertheless, Zhou et al. (2019) found that the spatial layout of forests, given a specific forest size, had no significant impact on pollution reduction within the administrative region. However, in their study, the UF form was primarily represented by its overall layout in the region, and no specific UF form metrics were involved. Therefore, the pollution reduction capacity of the UF form identified in our study was influenced by the UF size, providing a valuable complement to the existing studies.

### Reduce pollutants by optimizing UF form based on UF size thresholds

The influence of UF on  $\text{PM}_{2.5}$  and  $\text{O}_3$  concentrations has garnered sustained attention. This study takes UF size and form as two grips, focusing on the threshold effect of UF size on UF's pollution reduction capacity. It adds a new perspective

**Table 4** Partial results of threshold regression models

Pollutant	UF form metric	UF size value (PFO)	Coefficient
PM <sub>2.5</sub>	AWMSI	[0.000, 13.887]	4.756***
		(13.887, 100.000)	-1.236***
		[0.000, 3.105]	41.981***
	PD	(3.105, 45.228]	23.063***
		(45.228, 100.000)	14.199***
	SPLIT	[0.000, 3.136]	0.000**
		(3.136, 45.228]	-0.001***
		(45.228, 100.000)	-1.015***
	COHESION	[0.000, 45.228]	-0.028
		(45.228, 100.000)	-0.283***
O <sub>3</sub>	AWMSI	[0.000, 14.741]	-5.198***
		(14.741, 100.000)	1.043**
	PD	[0.000, 3.409]	-28.191***
		(3.409, 100.000)	-10.308***
	SPLIT	[0.000, 3.062]	-0.000***
		(3.062, 18.109]	0.001***
		(18.109, 100.000)	0.299***
	COHESION	[0.000, 3.331]	0.043
		(3.331, 100.000)	0.309***

(1) Three-hundred bootstrap replications are employed for each bootstrap test to calculate the P\_value; (2) Regarding the significance level, \* represents  $P_{\text{value}} < 0.1$ ; \*\* represents  $P_{\text{value}} < 0.01$ ; \*\*\* represents  $P_{\text{value}} < 0.001$

by considering the combined effects of UF size and form, providing potential pathways for pollutant reduction through the optimization of UF form based on size thresholds in practical applications. It is important to note that this study does not fully consider the interaction mechanisms of pollutants. Specifically, our analysis is based on extrapolating from the observed correlations between UF and pollutants to infer potential mechanisms and planning guidance, while also simply comparing analysis results of two pollutants. While this approach meets the research objectives, future studies could incorporate additional mechanisms involved in air pollution formation.

Established studies have explored the mechanisms through which UF influences PM<sub>2.5</sub> concentrations. On the one hand, vegetation can directly deposit and absorb particulate matter (Abhijith et al. 2017); On the other hand, vegetation as a whole can alter wind flow and turbulence or induce localized inversions, thereby hindering or facilitating pollutant dispersion (Santiago and Rivas 2021). This study further incorporates a size and form perspective into the above mechanisms. Specifically, we infer that the threshold for vegetation to develop scale effects through agglomeration is relatively low (nearly 3.1%), at which point it mainly plays the role of adsorption for PM<sub>2.5</sub> reduction. As UF size continues to increase thereafter, relatively small-area patches with a scattered layout

(when UF size > 3.1%) and irregularly shaped (when UF size > 13.9%) may decrease UF integrity, thereby reducing the uncertainty associated with their impact on the local climate. This finding is partially supported by previous studies. For example, Yang et al. (2021) found that small-area patches had a higher rate of compositional turnover for woody plants. This suggests that distribution patterns of small patches, which align with scale effects, can simultaneously reduce pollution and conserve UF diversity. Meanwhile, complex shapes can increase the interaction between UF and built-up areas to strengthen UF's role in mitigating PM<sub>2.5</sub>, which meets the finds of Chen et al. (2017) and Wang et al. (2022). Further, the above phenomenon may indicate that UF requires a smaller scale of aggregation for effective PM<sub>2.5</sub> adsorption than for influencing the local climate. This warrants further exploration in future studies.

Regarding mitigating O<sub>3</sub>, UF can reduce ozone primarily through dry deposition, while also indirectly generating ozone by emitting BVOCs (Taha et al. 2016). Based on our results, we further inferred that integrating vegetation elements into concentrated, regular UF patches is essential for enhanced dry deposition in the YRD. However, the ability of vegetation to release BVOCs is less influenced by the degree of agglomeration. Similarly, the study by Han et al. (2024) in Xi'an, China, found that vegetation can more readily release BVOCs, thereby driving O<sub>3</sub> concentrations higher in summer. Peng et al. (2024) found that the higher vegetation coverage guaranteed a more effective dry deposition of O<sub>3</sub>. Reviewing the combined effects of UF size and form in this study: When the UF size is below 14.7%, small UF patches tend to generate ozone by emitting BVOCs. In this case, scattered UF patches with complex shapes are required to mitigate the scale effect. When UF size exceeds 14.7%, vegetation begins to more effectively absorb ozone through dry deposition, suggesting that UF patches should form more regular shapes. However, when UF size surpasses 18.1%, UF patches should be aggregated to minimize BVOC emissions into built-up areas.

It can be seen that the strategies for mitigating PM<sub>2.5</sub> and O<sub>3</sub> differ when the UF size is relatively small. However, the optimal adjustments for the UF form to reduce both pollutants tend to converge as the size approaches a saturation point. Specifically, once UF size reaches a certain threshold (nearly 45.2%), more concentrated and continuous UF patches effectively manage both pollutants. At this stage, previously fragmented and irregularly shaped UF patches should be connected to form a cohesive whole, further strengthening the regional UF network (Teng et al. 2016). This phenomenon could serve as a support for the implementation of sustainable afforestation (Wang et al. 2024).

## Limitations and prospects

The study acknowledges several limitations. Firstly, the vegetation characteristics within UF play a crucial role in determining their effectiveness in mitigating pollution (Manes et al. 2012; Yin et al. 2022). The YRD was selected as the study area to address this due to its relatively homogeneous climatic conditions and vegetation characteristics. Future research could incorporate more comprehensive spatiotemporal big data on agroforestry for a broader analysis. Secondly, air pollution exhibits substantial temporal variability (Fu et al. 2022). This study used annual average pollutant concentrations to represent pollution levels. That's because UF size and form remain stable within the same year, and government spatial planning policies are typically structured on an annual basis. While this approach aligns with practical considerations, it may overlook some important details. Future research could explore dynamic relationships between UF and pollutant concentrations with a more refined temporal approach.

## Conclusions

UF planning has been recognized as an effective strategy for reducing PM<sub>2.5</sub> and O<sub>3</sub>. However, as afforestation progresses, the potential for further enlarging UF size and its marginal ecological benefits diminish, making the optimization of UF form a more feasible way. This study further proposes that UF size has threshold effects on UF form to reduce PM<sub>2.5</sub> and O<sub>3</sub>, thereby UF form could be optimized based on UF size thresholds.

To test and explore this hypothesis, the study examined the relationship between UF size, form, and pollutant concentrations across 305 counties in the YRD from 2014 to 2022, utilizing the panel threshold regression model. The threshold effects of UF size were further discussed. The main results are as follows:

- (1) The relationships between UF form and pollutants vary across different UF size intervals, influenced by the threshold effect of UF size. Specifically, a double threshold effect was observed in three relationships: between PD and PM<sub>2.5</sub>, between SPLIT and PM<sub>2.5</sub>, and between SPLIT and O<sub>3</sub>. In contrast, other relationships exhibit a single threshold effect.
- (2) The threshold values of UF size in these relationships are typically around 3%, 14%, and 45%. The study explains the phenomenon from the perspective of scale effects and diminishing marginal returns.
- (3) The correlations between UF form metrics and PM<sub>2.5</sub> are generally inverse to those with O<sub>3</sub>. The study sug-

gests that this is related to the different mechanisms through which UF influences the two pollutants.

- (4) When UF size is smaller than 45%, dispersed and complex-shaped UF patches could help reduce PM<sub>2.5</sub>, while O<sub>3</sub> reduction is more effective with regular and concentrated UF patches. Once UF size exceeds 45%, a continuous regional UF network becomes more advantageous for managing PM<sub>2.5</sub>-O<sub>3</sub> composite pollution.

**Supplementary Information** The online version contains supplementary material available at <https://doi.org/10.1007/s11869-025-01722-7>.

**Acknowledgements** The study doesn't involve human or animal subjects.

**Author contributions** *Xin Chen*: Conceptualization, Methodology, Formal analysis, Data curation, Visualization, Writing-Original draft preparation, Writing- Reviewing and Editing; *Fang Wei*: Supervision, Writing- Reviewing and Editing.

**Funding** The authors declare that no funds, grants, or other support were received during the preparation of this manuscript.

**Data availability** The datasets generated during and/or analyzed during the current study are not publicly available but are available from the corresponding author on reasonable request.

## Declarations

**Competing interests** The authors have no relevant financial or non-financial interests to disclose.

## References

- Abhijith KV, Kumar P, Gallagher J et al (2017) Air pollution abatement performances of green infrastructure in open road and built-up street canyon environments – A review. *Atmos Environ* 162:71–86. <https://doi.org/10.1016/j.atmosenv.2017.05.014>
- An Y, Dang Y, Wang J et al (2023) Identification of heavily polluted areas based on a novel grey integrated incidence model: A case study of the Yangtze River Delta, China. *Sustain Cities Soc* 92:104466. <https://doi.org/10.1016/j.scs.2023.104466>
- Cai L, Zhuang M, Ren Y (2020) A landscape scale study in South-east China investigating the effects of varied green space types on atmospheric PM2.5 in mid-winter. *Urban For Urban Green* 49:126607. <https://doi.org/10.1016/j.ufug.2020.126607>
- Cao W, Zhou W, Yu W, Wu T (2024) Combined effects of urban forests on land surface temperature and PM2.5 pollution in the winter and summer. *Sustain Cities Soc* 104:105309. <https://doi.org/10.1016/j.scs.2024.105309>
- Chen WY, Li X (2021) Urban forests' recreation and habitat potentials in China: A nationwide synthesis. *Urban for Urban Green* 66:127376. <https://doi.org/10.1016/j.ufug.2021.127376>
- Chen X, Wei F (2024) Impact of territorial spatial landscape pattern on PM2.5 and O<sub>3</sub> concentrations in the Yangtze River delta urban agglomeration: Exploration and planning strategies. *J Clean Prod* 452:142172. <https://doi.org/10.1016/j.jclepro.2024.142172>
- Chen Y-S, Shih C-Y, Chang C-H (2013) Patents and market value in the U.S. pharmaceutical industry: new evidence from panel threshold

- regression. *Scientometrics* 97:161–176. <https://doi.org/10.1007/s11192-013-0999-3>
- Chen L, Liu C, Zhang L et al (2017) Variation in Tree Species Ability to Capture and Retain Airborne Fine Particulate Matter (PM<sub>2.5</sub>). *Sci Rep* 7:3206. <https://doi.org/10.1038/s41598-017-03360-1>
- Deng T, Shao S, Yang L, Zhang X (2014) Has the transport-led economic growth effect reached a peak in China? A panel threshold regression approach. *Transportation* 41:567–587. <https://doi.org/10.1007/s11116-013-9503-4>
- Deng C, Jiang X, Tan Z, Nie T (2024) Spatiotemporal variation of hydrological connectivity and its threshold effects on flood dynamics: An examination in the arid and semi-arid regions, China. *Sci Total Environ* 935:173406. <https://doi.org/10.1016/j.scitotenv.2024.173406>
- Du S, He C, Zhang L et al (2024) Policy implications for synergistic management of PM<sub>2.5</sub> and O<sub>3</sub> pollution from a pattern-process-sustainability perspective in China. *Sci Total Environ* 916:170210. <https://doi.org/10.1016/j.scitotenv.2024.170210>
- Duan W, Wang X, Cheng S, Wang R (2022) Regional division and influencing mechanisms for the collaborative control of PM<sub>2.5</sub> and O<sub>3</sub> in China: A joint application of multiple mathematic models and data mining technologies. *J Clean Prod* 337:130607. <https://doi.org/10.1016/j.jclepro.2022.130607>
- Escobedo FJ, Nowak DJ (2009) Spatial heterogeneity and air pollution removal by an urban forest. *Landsc Urban Plan* 90:102–110. <https://doi.org/10.1016/j.landurbplan.2008.10.021>
- Fan H, Yu Z, Yang G et al (2019) How to cool hot-humid (Asian) cities with urban trees? An optimal landscape size perspective. *Agric for Meteorol* 265:338–348. <https://doi.org/10.1016/j.agrformet.2018.11.027>
- Feng R, Fang X (2022) China's pathways to synchronize the emission reductions of air pollutants and greenhouse gases: Pros and cons. *Resour Conserv Recycl* 184:106392. <https://doi.org/10.1016/j.resconrec.2022.106392>
- Fu W, Qiao Y, Que C et al (2022) The characteristics of ambient air quality in urban forest areas and other urban areas of Fuzhou city, China. *Environ Dev Sustain* 24:9500–9518. <https://doi.org/10.1007/s10668-021-01837-8>
- Han L, Zhou W, Li W, Qian Y (2022) Challenges in continuous air quality improvement: An insight from the contribution of the recent clean air actions in China. *Urban Clim* 46:101328. <https://doi.org/10.1016/j.uclim.2022.101328>
- Han L, Zhang R, Wang J, Cao S-J (2024) Spatial synergistic effect of urban green space ecosystem on air pollution and heat island effect. *Urban Clim* 55:101940. <https://doi.org/10.1016/j.uclim.2024.101940>
- Hansen BE (1999) Threshold effects in non-dynamic panels: Estimation, testing, and inference. *J Econom* 93:345–368. [https://doi.org/10.1016/S0304-4076\(99\)00025-1](https://doi.org/10.1016/S0304-4076(99)00025-1)
- Hansen BE (2000) Sample Splitting and Threshold Estimation. *Econometrica* 68:575–603. <https://doi.org/10.1111/1468-0262.00124>
- Hu D, Wu J, Tian K et al (2017) Urban air quality, meteorology and traffic linkages: Evidence from a sixteen-day particulate matter pollution event in December 2015, Beijing. *J Environ Sci* 59:30–38. <https://doi.org/10.1016/j.jes.2017.02.005>
- Hu T, Li X, Gong P et al (2020) Evaluating the effect of plain afforestation project and future spatial suitability in Beijing. *Sci China Earth Sci* 63:1587–1598. <https://doi.org/10.1007/s11430-019-9636-0>
- Huo T, Cao R, Du H et al (2021) Nonlinear influence of urbanization on China's urban residential building carbon emissions: New evidence from panel threshold model. *Sci Total Environ* 772:145058. <https://doi.org/10.1016/j.scitotenv.2021.145058>
- Kong F, Yin H, James P et al (2014) Effects of spatial pattern of greenspace on urban cooling in a large metropolitan area of eastern China. *Landsc Urban Plan* 128:35–47. <https://doi.org/10.1016/j.landurbplan.2014.04.018>
- Konijnendijk CC (2003) A decade of urban forestry in Europe. *For Policy Econ* 5:173–186. [https://doi.org/10.1016/S1389-9341\(03\)00023-6](https://doi.org/10.1016/S1389-9341(03)00023-6)
- Li L, Chen CH, Huang C et al (2012) Process analysis of regional ozone formation over the Yangtze River Delta, China using the Community Multi-scale Air Quality modeling system. *Atmospheric Chem Phys* 12:10971–10987. <https://doi.org/10.5194/acp-12-10971-2012>
- Li J, Han L, Zhou W et al (2023) Uncertainties in research between urban landscape and air quality: summary, demonstration, and expectation. *Landsc Ecol* 38:2475–2485. <https://doi.org/10.1007/s10980-023-01744-5>
- Li R, Gao Y, Xu J et al (2023) Impact of clean air policy on criteria air pollutants and health risks across China during 2013–2021. *J Geophys Res Atmospheres* 128:e2023JD038939. <https://doi.org/10.1029/2023JD038939>
- Li W, Chen Z, Li M et al (2023) Carbon emission and economic development trade-offs for optimizing land-use allocation in the Yangtze River Delta, China. *Ecol Indic* 147:109950. <https://doi.org/10.1016/j.ecolind.2023.109950>
- Li X, Jia B, Li T, Feng F (2023) Studying the spatial evolutionary behavior of urban forest patches from the perspective of pattern-process relationships. *Urban For Urban Green* 81:127861. <https://doi.org/10.1016/j.ufug.2023.127861>
- Lin Y, Yuan X, Zhai T, Wang J (2020) Effects of land-use patterns on PM<sub>2.5</sub> in China's developed coastal region: Exploration and solutions. *Sci Total Environ* 703:135602. <https://doi.org/10.1016/j.scitotenv.2019.135602>
- Lin H, Zhu J, Jiang P et al (2022) Assessing drivers of coordinated control of ozone and fine particulate pollution: Evidence from Yangtze River Delta in China. *Environ Impact Assess Rev* 96:106840. <https://doi.org/10.1016/j.eiar.2022.106840>
- Liu Y, Zhou Y (2021) Territory spatial planning and national governance system in China. *Land Use Policy* 102:105288. <https://doi.org/10.1016/j.landusepol.2021.105288>
- Liu Y, Li J, Yang Y (2018) Strategic adjustment of land use policy under the economic transformation. *Land Use Policy* 74:5–14. <https://doi.org/10.1016/j.landusepol.2017.07.005>
- Liu M, Wei D, Chen H (2022) Consistency of the relationship between air pollution and the urban form: Evidence from the COVID-19 natural experiment. *Sustain Cities Soc* 83:103972. <https://doi.org/10.1016/j.scs.2022.103972>
- Lu D, Xu J, Yue W et al (2020) Response of PM<sub>2.5</sub> pollution to land use in China. *J Clean Prod* 244:118741. <https://doi.org/10.1016/j.jclepro.2019.118741>
- Lu J, Li B, Li H, Al-Barakani A (2021) Expansion of city scale, traffic modes, traffic congestion, and air pollution. *Cities* 108:102974. <https://doi.org/10.1016/j.cities.2020.102974>
- Manes F, Incerti G, Salvatori E et al (2012) Urban ecosystem services: tree diversity and stability of tropospheric ozone removal. *Ecol Appl* 22:349–360. <https://doi.org/10.1890/11-0561.1>
- Mo Y, Kim HG, Huber PR et al (2019) Influences of planning unit shape and size in landscapes dominated by different land-cover types on systematic conservation planning. *Glob Ecol Conserv* 20:e00739. <https://doi.org/10.1016/j.gecco.2019.e00739>
- Ouyang X, Shao Q, Zhu X et al (2019) Environmental regulation, economic growth and air pollution: Panel threshold analysis for OECD countries. *Sci Total Environ* 657:234–241. <https://doi.org/10.1016/j.scitotenv.2018.12.056>
- Pathak RK, Wu WS, Wang T (2009) Summertime PM<sub>2.5</sub> ionic species in four major cities of China: nitrate formation in an ammonia-deficient atmosphere. *Atmospheric Chem Phys* 9:1711–1722. <https://doi.org/10.5194/acp-9-1711-2009>

- Peng J, Xie P, Liu Y, Ma J (2016) Urban thermal environment dynamics and associated landscape pattern factors: A case study in the Beijing metropolitan region. *Remote Sens Environ* 173:145–155. <https://doi.org/10.1016/j.rse.2015.11.027>
- Peng J, Liu Q, Xu Z et al (2020) How to effectively mitigate urban heat island effect? A perspective of waterbody patch size threshold. *Landsc Urban Plan* 202:103873. <https://doi.org/10.1016/j.landurbplan.2020.103873>
- Peng H, Shao S, Xu F et al (2024) Dry Deposition in Urban Green Spaces: Insights from Beijing and Shanghai. *Forests* 15:1286. <https://doi.org/10.3390/f15081286>
- Qi G, Che J, Wang Z (2023) Differential effects of urbanization on air pollution: Evidences from six air pollutants in mainland China. *Ecol Indic* 146:109924. <https://doi.org/10.1016/j.ecolind.2023.109924>
- Qu Y, Wang T, Yuan C et al (2023) The underlying mechanisms of PM2.5 and O<sub>3</sub> synergistic pollution in East China: Photochemical and heterogeneous interactions. *Sci Total Environ* 873:162434. <https://doi.org/10.1016/j.scitotenv.2023.162434>
- Ran P, Hu S, Frazier AE et al (2023) The dynamic relationships between landscape structure and ecosystem services: An empirical analysis from the Wuhan metropolitan area, China. *J Environ Manage* 325:116575. <https://doi.org/10.1016/j.jenvman.2022.116575>
- Santiago J-L, Rivas E (2021) Advances on the influence of vegetation and forest on urban air quality and thermal comfort. *Forests* 12:1133. <https://doi.org/10.3390/f12081133>
- Shen Z, Zhang Z, Cui L et al (2023) Coordinated change of PM2.5 and multiple landscapes based on spatial coupling model: Comparison of inland and waterfront cities. *Environ Impact Assess Rev* 102:107194. <https://doi.org/10.1016/j.eiar.2023.107194>
- Shih W (2017) Greenspace patterns and the mitigation of land surface temperature in Taipei metropolis. *Habitat Int* 60:69–80. <https://doi.org/10.1016/j.habitatint.2016.12.006>
- Silveira C, Amaral FG, Dias ATC et al (2024) The importance of private gardens and their spatial composition and configuration to urban heat island mitigation. *Sustain Cities Soc* 112:105589. <https://doi.org/10.1016/j.scs.2024.105589>
- Taha H, Wilkinson J, Bornstein R et al (2016) An urban-forest control measure for ozone in the Sacramento, CA Federal Non-Attainment Area (SFNA). *Sustain Cities Soc* 21:51–65. <https://doi.org/10.1016/j.scs.2015.11.004>
- Teng M, Zhou Z, Wang P et al (2016) Geotechnology-Based Modeling to Optimize Conservation of Forest Network in Urban Area. *Environ Manage* 57:601–619. <https://doi.org/10.1007/s00267-015-0642-6>
- Toledo-Garibaldi M, Gallardo-Hernández C, Ulian T, Toledo-Aceves T (2023) Urban forests support natural regeneration of cloud forest trees and shrubs, albeit with limited occurrence of late-successional species. *For Ecol Manag* 546:121327. <https://doi.org/10.1016/j.foreco.2023.121327>
- Tong H (1983) Threshold Models in Non-linear Time Series Analysis. Springer, New York, NY
- Vaz Monteiro M, Doick KJ, Handley P, Peace A (2016) The impact of greenspace size on the extent of local nocturnal air temperature cooling in London. *Urban For Urban Green* 16:160–169. <https://doi.org/10.1016/j.ufug.2016.02.008>
- Wang C, Guo M, Jin J et al (2022) Does the spatial pattern of plants and green space affect air pollutant concentrations? Evidence from 37 garden Cities in China. *Plants* 11:2847. <https://doi.org/10.3390/plants11212847>
- Wang C, Jin J, Davies C, Chen WY (2024) Urban forests as nature-based solutions: a comprehensive overview of the national Forest City action in China. *Curr for Rep* 10:119–132. <https://doi.org/10.1007/s40725-024-00213-9>
- Wei J, Li Z, Lyapustin A et al (2021) Reconstructing 1-km-resolution high-quality PM2.5 data records from 2000 to 2018 in China: spatiotemporal variations and policy implications. *Remote Sens Environ* 252:112136. <https://doi.org/10.1016/j.rse.2020.112136>
- Wei J, Li Z, Li K et al (2022) Full-coverage mapping and spatiotemporal variations of ground-level ozone (O<sub>3</sub>) pollution from 2013 to 2020 across China. *Remote Sens Environ* 270:112775. <https://doi.org/10.1016/j.rse.2021.112775>
- Wu J, Wang Y, Liang J, Yao F (2021) Exploring common factors influencing PM2.5 and O<sub>3</sub> concentrations in the Pearl River Delta: Tradeoffs and synergies. *Environ Pollut* 285:117138. <https://doi.org/10.1016/j.envpol.2021.117138>
- Wu H, Guo B, Guo T et al (2024) A study on identifying synergistic prevention and control regions for PM2.5 and O<sub>3</sub> and exploring their spatiotemporal dynamic in China. *Environ Pollut* 341:122880. <https://doi.org/10.1016/j.envpol.2023.122880>
- Xiao Q, Geng G, Liang F et al (2020) Changes in spatial patterns of PM2.5 pollution in China 2000–2018: Impact of clean air policies. *Environ Int* 141:105776. <https://doi.org/10.1016/j.envint.2020.105776>
- Xu C, Dong L, Yu C et al (2020) Can forest city construction affect urban air quality? The evidence from the Beijing-Tianjin-Hebei urban agglomeration of China. *J Clean Prod* 264:121607. <https://doi.org/10.1016/j.jclepro.2020.121607>
- Yang J, Yang J, Xing D et al (2021) Impacts of the remnant sizes, forest types, and landscape patterns of surrounding areas on woody plant diversity of urban remnant forest patches. *Urban Ecosyst* 24:345–354. <https://doi.org/10.1007/s11252-020-01040-z>
- Yang J, Cen C, Wang Z, Jian M (2024) Impacts of spatiotemporal urban expansion on the species richness and functional traits of adults and sapling woody trees and shrubs of urban remnant forest patches. *Ecol Indic* 166:112498. <https://doi.org/10.1016/j.ecolind.2024.112498>
- Yang J, Huang X (2023) The 30 m annual land cover datasets and its dynamics in China from 1985 to 2022
- Yin S, Chen D, Zhang X, Yan J (2022) Review on the multi-scale interactions of urban forests and atmospheric particles: Affecting factors are scale-dependent among tree, stand and region. *Urban For Urban Green* 78:127789. <https://doi.org/10.1016/j.ufug.2022.127789>
- Yu Z, Yang G, Zuo S et al (2020) Critical review on the cooling effect of urban blue-green space: A threshold-size perspective. *Urban For Urban Green* 49:126630. <https://doi.org/10.1016/j.ufug.2020.126630>
- Zhai C, Bao G, Zhang D, Sha Y (2022) Urban forest locations and patch characteristics regulate PM2.5 mitigation capacity. *Forests* 13:1408. <https://doi.org/10.3390/f13091408>
- Zhang X, Du J, Zhang L et al (2020) Impact of afforestation on surface ozone in the North China Plain during the three-decade period. *Agric For Meteorol* 287:107979. <https://doi.org/10.1016/j.agrifo.2020.107979>
- Zhang J, Wang J, Sun Y et al (2022) Insights from ozone and particulate matter pollution control in New York City applied to Beijing. *Npj Clim Atmospheric Sci* 5:1–7. <https://doi.org/10.1038/s41612-022-00309-8>
- Zhao X, Huang G (2022) Urban watershed ecosystem health assessment and ecological management zoning based on landscape pattern and SWMM simulation: A case study of Yangmei River Basin. *Environ Impact Assess Rev* 95:106794. <https://doi.org/10.1016/j.eiar.2022.106794>
- Zhao H, Chen K, Liu Z et al (2021) Coordinated control of PM2.5 and O<sub>3</sub> is urgently needed in China after implementation of the “Air pollution prevention and control action plan.” *Chemosphere* 270:129441. <https://doi.org/10.1016/j.chemosphere.2020.129441>
- Zhao X, Zhang Z, Xu J et al (2023) Impacts of aerosol direct effects on PM2.5 and O<sub>3</sub> respond to the reductions of different primary

- emissions in Beijing-Tianjin-Hebei and surrounding area. *Atmos Environ* 309:119948. <https://doi.org/10.1016/j.atmosenv.2023.119948>
- Zheng Y, Li S, Zou C et al (2019) Analysis of PM2.5 concentrations in Heilongjiang Province associated with forest cover and other factors. *J For Res* 30:269–276. <https://doi.org/10.1007/s11676-018-0640-7>
- Zhou ZC, Wang J (2022) Evolution of landscape dynamics in the Yangtze River Delta from 2000 to 2020. *J Water Clim Change* 13:1241–1256. <https://doi.org/10.2166/wcc.2022.307>
- Zhou Y, Liu H, Zhou J, Xia M (2019) GIS-based urban afforestation spatial patterns and a strategy for PM2.5 removal. *Forests* 10:875. <https://doi.org/10.3390/f10100875>
- Zhu Z, Wang G, Dong J (2019) Correlation analysis between land use/cover change and air pollutants—a case study in Wuyishan City. *Energies* 12:2545. <https://doi.org/10.3390/en12132545>

**Publisher's Note** Springer Nature remains neutral with regard to jurisdictional claims in published maps and institutional affiliations.

Springer Nature or its licensor (e.g. a society or other partner) holds exclusive rights to this article under a publishing agreement with the author(s) or other rightsholder(s); author self-archiving of the accepted manuscript version of this article is solely governed by the terms of such publishing agreement and applicable law.